Simultaneous determination of absolute and relative permeabilities ☆

Randi Valestrand [a,*], Alv-Arne Grimstad [b], Kristofer Kolltveit [a], Geir Nævdal [b],
Jan-Erik Nordtvedt [a]

[a] *Department of Physics, University of Bergen, Allegt. 55, N-5007 Bergen, Norway*
[b] *RF-Rogaland Research, Thormøhlensgt. 55, N-5008 Bergen, Norway*

Abstract

Data from core analyses, such as residual oil saturation and relative permeabilities, are of great importance for proper exploitation of the petroleum resources. Such quantities are typically determined through interpretation of data acquired during some flooding experiment. In such determinations, the absolute permeabilities are typically represented by a single average value, i.e., the core is assumed homogeneous and isotropic. Recent studies, however, show that the validity of such assumptions can be questioned. When using such assumptions analyzing flooding data, the derived relative permeabilities will depend on the actual core sample heterogeneity, i.e., the variation and distribution of the absolute permeability in the core. A better option would therefore be to determine the absolute and relative permeabilities simultaneously from the data, thereby accounting for heterogeneity effects. In this paper we describe and test a method for such determinations, and discuss some results. © 2002 Éditions scientifiques et médicales Elsevier SAS. All rights reserved.

Keywords: Porous media; Fluid flow; Heterogeneous media; Inverse problem; Relative permeability; Absolute permeability

1. Introduction

The relative permeabilities are saturation dependent functions describing the fluid flow when several phases are present and flowing in a porous media. Accurate estimates of these functions are of great importance for proper exploitation of the petroleum resources. The functions are, however, inaccessible to direct measurement, and are typically determined through interpretation of data acquired during some two-phase flow experiment on small samples (i.e., cores) of the porous media. Over the past more than 10 years, an inverse methodology, in which basically a core flow simulator is utilized for reconciliation of laboratory data, has been developed, tested, and reported in a series of papers [6,10,15]. In this approach, the relative permeability and capillary pressure functions (collectively referred to as flow functions) are estimated simultaneously. The method has proven to be successful, provided that all the important physical processes are included in the simulator.

For the most common methods used when determining the flow functions, the absolute permeability is typically represented by a single average value, i.e., the core is assumed homogeneous and isotropic. Recent studies, however, show that the validity of such assumptions can be questioned [17]. Reservoirs and also small core samples may indeed be heterogeneous and anisotropic, and the data collected from flooding experiments are usually influenced by the effect caused by this. While the collected data will be influenced by the actual core sample heterogeneity, assuming homogeneity when determining the flow functions may inflict serious estimation errors. The effect and importance of these errors have been studied in some detail, and the results show that the modeling error associated with the homogeneity assumption frequently result in highly erroneous estimates of the flow functions [17].

A better option would therefore be to include the variation of absolute permeability when estimating the flow functions. We have developed and tested a method that does this. In the estimation procedure we allow for spatial distribution of the absolute permeability.

Nomenclature

a	spline coefficients		R	number of runs
B	spline basis function		S	saturation
b	parameter vector		W	weighting matrix
c	parameter vector		**x**	parameter vector
D	basis matrix		**Y**	vector of data
$E(\cdot)$	expectation		Y	data
F	model output vector		**y**	spline knot vector
F	model output		**e**	residual vector
G	sensitivity matrix		e	residual
J	objective function		μ	viscosity . . . . Poise = g·s^{-1}·cm^{-1}
k	absolute permeability . . . . . . Darcy $\approx 10^{-12}$ m^2		ϕ	porosity
K	vector of absolute permeabilities		σ	standard deviation
k_r	relative permeability			
m	number of data		*Subscripts and superscripts*	
n	number of parameters			
P_c	capillary pressure . . . . Pa = N/m^2		o	oil
p	pressure . . . . Pa		w	water

In this paper, we describe and test this method for simultaneous determination of absolute and relative permeabilities, and discuss some results. To the best of our knowledge, this is the first time a model for simultaneous determination of absolute and relative permeabilities from displacement data is presented.

We focus our initial investigation on simultaneous estimation of absolute and relative permeabilities on the composite core case. A composite core is a sample consisting of two or more porous media samples butted together. In core analysis this is done to decrease the importance of end effects, and decrease the relative error in the measured production data [12]. The absolute permeability of the composite is usually represented by a mean value when estimating the flow functions. Recent findings indicate that large errors may result if the permeability of the individual samples in the composite deviate from the mean permeability value [17].

By simultaneous estimation of absolute and relative permeabilities, we account for a potential variation of the absolute permeability in the core sample. The data used to perform such estimations must contain information about the heterogeneity as well as the fluid flow of several phases. This is achieved by utilizing data from steady-state, two-phase flow experiments on composite cores [15]. In a steady-state experiment, two immiscible phases are injected simultaneous in rate steps. At each rate step change the amount of one of the phases injected is reduced, and at the last rate step only one phase is injected. Production and pressure data are collected during the equilibration at each rate fraction. The absolute and relative permeabilities are estimated from these data through an inverse problem [15].

When testing a method, it would be beneficial to know the correct answer to the exercise. If experimental data is used, we do not know the answer. When utilizing synthetic experimental data, however, we know the correct answer before we start the estimation process. In this paper we utilize synthetic experimental data since these provide a more thorough check of the method. The synthetic experimental data are produced by a 1D core flow simulator [7] with a set of true relative permeability curves and true permeability variation implemented. The flow scenario described above is simulated to produce synthetic pressure and production data. Here, we will demonstrate the simultaneous estimation method by three examples, utilizing data from three independent synthetic experiments. First, a description of the mathematical model is provided.

2. Mathematical model

2.1. The forward model

Flow in porous media occurs through an interconnected irregular network of pores within a solid. Background material and model equations for general multi-phase flow in porous media can be found, e.g., in the book by Aziz and Settari [1].

In core analysis, simplified versions of the general porous-media flow equations are used. Assuming constant fluid densities, 1D flow, and no gravity effects, the flow of two immiscible fluid phases (e.g., oil and water) through porous media is essentially described by

$$\phi \frac{\partial S_w}{\partial t} = \frac{\partial}{\partial x}\left(\frac{k k_{rw}(S_w)}{\mu_w}\frac{\partial p_w}{\partial x}\right) \tag{1}$$

$$\phi \frac{\partial S_o}{\partial t} = \frac{\partial}{\partial x}\left(\frac{k k_{ro}(S_w)}{\mu_o}\frac{\partial p_o}{\partial x}\right) \tag{2}$$

$$p_{\mathrm{o}} - p_{\mathrm{w}} = P_{\mathrm{c}}(S_{\mathrm{w}}) \tag{3}$$

$$S_{\mathrm{o}} + S_{\mathrm{w}} = 1 \tag{4}$$

Together with boundary and initial conditions, Eqs. (1)–(4) provide a mathematical model of 1D two-phase fluid flow in porous media.

If the terms in these equations were known, the model output, **F**, would correspond to the experimental data, **Y**, acquired from a corresponding experiment. Examples of such data (in core analysis) are: Fluid production, pressure drop, in-situ saturation, in-situ pressure, and in-situ saturation profiles.

The absolute and relative permeability are included in Eqs. (1)–(4) but are generally not known. To be able to predict reservoir behavior we need these functions. The solution is to estimate the absolute and relative permeability through an inverse problem.

2.2. The inverse problem

Let **Y** be the vector containing the measured experimental data. Let **F**(**b**) be the vector containing the corresponding values calculated from the mathematical model, where **b** is a vector of unknown adjustable parameters. The unknown parameters are varied until the **Y** and **F** are close in some sense.

An objective function is formulated as a weighted sum of squared differences between the measured data and the corresponding simulated values. In the estimation process, one seeks to minimize the objective function,

$$J(\mathbf{b}) = \left[\mathbf{Y} - \mathbf{F}(\mathbf{b}) \right]^{\mathrm{T}} W \left[\mathbf{Y} - \mathbf{F}(\mathbf{b}) \right] \tag{5}$$

the idea being that the simulated data should reconcile those actually measured. The weighting matrix W is selected according to statistical criteria so that, with appropriate choices of the mathematical model and the functional representation of the unknowns (e.g., absolute and relative permeability), maximum-likelihood estimates are obtained [2,18]. It is assumed that the model is correct, and that the measurement errors are independent and additive, so that W can be taken to be a diagonal matrix with entries equal to the inverse of the estimated variances of the data measurement errors.

We account for physical constraints of the unknown functions, such as monotonous relative permeability functions and nonnegative absolute permeability, by including linear inequality constraints on the unknown parameters. The value of **b** that minimizes Eq. (5) is obtained by an implementation of the Levenberg–Marquardt optimization algorithm, which incorporates the linear inequality constraints [4,18].

Next we consider the representation of the unknown functions.

3. Property representation

The first step in solving the inverse problem is to select an adequate functional representation for the unknown absolute and relative permeability functions.

The relative permeabilities are saturation dependent continuous functions, defined between zero and one, describing the phases' ability to flow through the porous media. For example, the oil relative permeability curve equals unity if the porous media is fully saturated with mobile oil, and it equals zero when no oil is mobile. Between zero and unity, the functions' value is dependent on the pore space available for oil, i.e., the oil saturation. The saturation is given in fractions, e.g., if the porous media is fully saturated with oil then $S_{\mathrm{o}} = 1$.

In this work quadratic B-spline functions [13] are used to represent the relative permeability functions. The B-spline representation for the two-phase relative permeability functions is given by

$$k_{\mathrm{ri}}(S_{\mathrm{w}}) = \sum_{j=1}^{N_i} a_j^i B_j^m \left(S_{\mathrm{w}}, \mathbf{y}^i \right) \tag{6}$$

The functions are defined on $0 \leqslant S_{\mathrm{w}} \leqslant 1$, and are specified by the order m, the spline coefficients a_j^i, and the extended partition $\mathbf{y}^i$. The vector of unknown parameters, **x**, composed of the coefficients within the spline representation of the relative permeability functions is given by

$$\mathbf{x} = \left[a_1^{\mathrm{o}}, \ldots, a_{N_{\mathrm{o}}}^{\mathrm{o}}, a_1^{\mathrm{w}}, \ldots, a_{N_{\mathrm{w}}}^{\mathrm{w}} \right] \tag{7}$$

The unknown parameters **x** of the relative permeability representation is used as the vector **b** in Eq. (5) when the relative permeabilities are estimated.

The absolute permeability is defined as the ability of the porous media to allow flow through its pores. It is actually a tensor of the second rank due to the heterogeneous and anisotropic nature of porous media. In this work k is treated as a scalar, i.e., we consider an isotropic media.

To estimate the absolute permeability, k, of the porous media we represent it by hierarchical multiscale basis functions [3]. With this representation the various terms in the property function series represents variation on different length scales. A parameter vector, **c**, is related to the permeability through the relationship

$$\mathbf{K} = D\mathbf{c} \tag{8}$$

Here **K** is an n-vector where each entry represents the permeability in one of the n grid blocks, **c** is a j-vector of parameters, and D is an $n \times j$ matrix. With this representation the permeability has j degrees of freedom. Since there are only a finite number of grid blocks, the relationship between the basis functions and the permeability can be represented using an $n \times j$ matrix D. Each column of D represents one of the basis functions. The basis functions we use are quite similar to the Haar basis functions [3].

When estimating the absolute permeability in this work, **b** in Eq. (5) equals the parameter vector **c**.

4. Estimation method

4.1. Simultaneous estimation

We have combined the estimation of absolute and relative permeability by estimating the parameters **x** and **c** successively. First the relative permeabilities are estimated utilizing the harmonic mean value of the absolute permeability. (The harmonic mean value of the absolute permeability can easily be measured in a one-phase flow experiment, thus, the value is generally known in core analysis.) Then the absolute permeability is estimated, keeping the relative permeabilities fixed at their first estimate. We then return to the relative permeabilities, keeping the absolute permeability fixed at its latest estimate. This procedure is repeated until convergence. Thus, successively more accurate estimates for the absolute and the relative permeabilities are determined. Note that both the absolute and the relative permeabilities are estimated by the same estimation algorithm (solution of Eq. (5)).

4.2. Solution criteria

In general, large errors could be present in the estimates if they are achieved from inverse models incapable of reconciling the experimental data [6]. To discard solutions where the experimental data are not reconciled, solution criteria for validating estimates of absolute and relative permeabilities from laboratory data have been established [6, 16].

When utilizing the inverse methodology, there are two requirements that should be met to accept an estimate:

(1) The mathematical model on which the estimation procedure is based should include all the important physical effects encountered in the experiment.
(2) The estimates of the unknowns should be consistent with the data measured during the experiment.

To validate if these two requirements are met by a possible candidate solution of the inverse problem, statistical criteria [2,6,16,18] are utilized.

If the measurement noise are assumed random and uncorrelated with normal probability distribution and zero mean, the weighting matrix is taken to be a diagonal matrix with entries equal to the inverse estimated variances of the measurement noise. The objective function, Eq. (5), can then be written as $J(\mathbf{b}) = \sum_l (e_l(\mathbf{b})/\sigma_l)^2$ where $e_l(\mathbf{b})$ are the residuals. The residuals are defined as the m differences

$$e_k(\mathbf{b}) = Y_k - F_k(\mathbf{b}) \quad k = 1, \dots, m \tag{9}$$

where Y_k is an observation, and $F_k(\mathbf{b})$ is the corresponding value from the simulator output. From statistical calculations, the expected value of J, $E(J)$, should approach $m - n$, where m is the number of measurements, and n is the number of elements in $\mathbf{b}$ [2,19].

Even if the objective function approaches this limit, one should still check whether the residuals are biased or not. A statistical measure of this is to count the number of runs made by the time series of residuals [2]. The number of runs is the number of times the residuals change signs as one move through the data set. It can be defined as

$$R = \sum_{i=1}^{m-1} r_i \quad \text{where } r_i = \begin{cases} 1 & \text{if } e_{i+1} \cdot e_i < 0 \\ 0 & \text{otherwise} \end{cases} \tag{10}$$

For large m, and with the number of positive and negative residuals approximately equal, R will have an approximately normal distribution with an expected value, $E(R)$, equal to $m/2$.

We also compute the impact of measurement noise on the estimated functions. This is done by utilizing a linearized covariance analysis [16,19] in which the accuracy of the estimates is represented by confidence intervals.

4.3. Multiscale estimation

By using the multiscale representation of the absolute permeability, variation on many length scales can be accounted for. With such a basis for the functional space, the various terms in the coefficient function series represent variation on different length scales. The first term, basis function 1, represents a mean value on the domain of definition, while including more terms corresponds to representing variation on successively finer length scales.

Which basis functions and how many to include in the basis D, is not known a priori. We would like to reduce the value of the objective function J by increasing the resolution of the permeability in a proper way. Evaluating every possible choice by actually performing the minimization of Eq. (5) for all these choices is prohibitive. We choose the refinement based on projected objective function reduction calculated from the reduction potential for prospective choices. The reduction potential, f, is based on linearization of $\mathbf{F}$ [5,11], and is defined by

$$f(G, W, \mathbf{e}) = (\mathbf{e})^{\mathrm{T}} W G (G^{\mathrm{T}} W G)^{-1} G^{\mathrm{T}} W (\mathbf{e}) \tag{11}$$

where $G = \mathbf{F}'(\mathbf{c})$ is the sensitivity matrix and $\mathbf{e} = \mathbf{Y} - \mathbf{F}(\mathbf{c})$ is the residual vector. Note that the sensitivity matrix G depends on the choice of parameterization.

When extending the basis D, we would like to keep the uncertainty in the estimates low. Hence, a measure of the maximum uncertainty for the refinement is needed. We use the inverse of the minimum eigenvalue of the linearized information matrix, $G^{\mathrm{T}} W G$, of the parameters.

When evaluating the various refinement choices, we choose a method motivated by the L-curve methodology [8]. Thus, we plot the expected objective function as a function of expected uncertainty, and the refinement candidate corresponding to the lowest objective function is chosen if the uncertainty is sufficiently small.

4.4. Estimation algorithm

The simultaneous estimation method described in Section 4.1 can be explained in detail by the following estimation algorithm.

Initialization: as the first estimate of the permeability, use the harmonic mean value. Estimate the relative permeabilities while keeping the absolute permeability fixed at the harmonic mean value.

Estimate the permeability (using the current estimate of the relative permeability):

(1) Estimate a constant value of the permeability.
(2) Calculate all the possible refinement potentials by including one and two additional basis functions, in addition to the constant function. Set $N = 1$.
(3) While the best refinement potential with $N + 1$ additional basis functions is significantly better than the best refinement potential with N additional basis functions, compute the refinement potentials for $N + 2$ additional basis functions, and set $N = N + 1$.
(4) Find a final estimate of the absolute permeability with this relative permeability by performing a new estimation using the basis obtained in step 3.
(5) If the solution criteria (value of objective function and number of runs) are satisfied, or the current estimate is close to the previous final estimate of the permeability, do a final estimation of the relative permeability and stop.

Estimating the relative permeability: estimate the relative permeability. If the solution criteria are satisfied, stop, else return to step 1.

5. Results and discussion

The estimation procedure described above is tested on three synthetic examples. The true relative permeabilities, true capillary pressure, and experimental setup are the same for these three examples when simulated experimental data are produced. The true absolute permeability is different for the three examples.

All the cases studied are 1D due to simplicity. The estimation tool described above is extendable to deal with 2D cases, and real experimental data can be used. However, we choose to deal with simple cases initially to develop an understanding of the problem at hand, and also to perform a check of the estimation method.

Example 1. The true absolute permeability used in Example 1 is shown in Fig. 1. 32 equally sized grid blocks in the horizontal direction represent the 12.8 cm core. Grid blocks 1–11 have a true permeability of 50 mD, while grid blocks 12–32 have a true permeability of 100 mD.

The true relative permeability functions are shown in Fig. 2. All the grid blocks are represented by these relative permeability functions. The true capillary pressure is also equal for all the grid blocks. In practice the capillary pressure will vary in a heterogeneous core. We have here idealized the situation, to concentrate our initial studies on the effect of permeability alone.

Certain core and fluid properties are, together with the true functions implemented in the core flow model to produce synthetic experimental data. The core and fluid
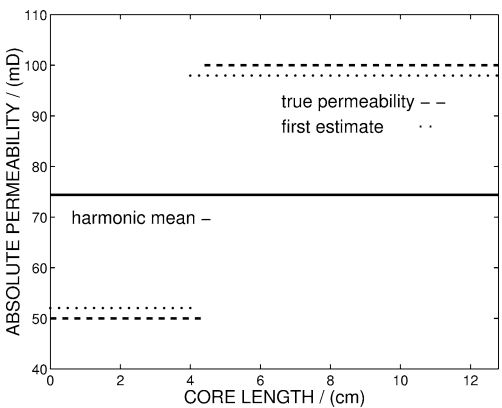

Fig. 1. Absolute permeability. The true distribution, the harmonic mean, and the first estimate (Example 1).
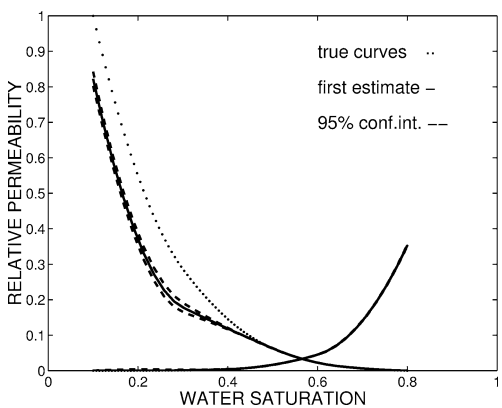

Fig. 2. Relative permeability. True curves, and first estimate with 95% confidence intervals (Example 1).

Table 1
Core flood simulator input

Core length (*x*-direction)	12.8 cm
No. of grid blocks (*x*-direction)	32
Water viscosity	0.85 cP
Oil viscosity	0.66 cP
Initial water saturation	10 %
Initial oil saturation	90 %
Porosity	30%
Oil injection rates [cc/min]	0.95, 0.5
Water injection rates [cc/min]	0.05, 0.5, 1.0

properties and the flow rates are listed in Table 1. A steady state experiment is simulated, where the saturation range is changed in steps due to the oil/water ratio injected. Similar experiments have been performed and reported earlier, see [14,15]. Gaussian noise with zero mean is then added to the data to simulate measurement errors. For the production data the standard deviation of the added noise is chosen to be 0.1 ml, and for the pressure data it is chosen to be 0.9 kPa. This is the size of typical measurement errors [14].

Figs. 3 and 4 show the synthetic oil production and pressure data used in the analysis of Example 1. The oil production and differential pressure shown in Fig. 3 are used when estimating the relative permeabilities. When estimating the absolute permeability we include the pressure data in Fig. 4 in addition to the oil production data in Fig. 3. In Fig. 4 P_a, P_b, P_c, and P_d are the pressures measured in grid blocks 1, 8, 24, and 32, respectively.

For all the relative permeability estimates both the water and the oil relative permeabilities are represented by five spline parameters.

When describing the simultaneous estimation procedure, we will refer to the steps in the estimation algorithm of Section 4.4. The estimation of absolute permeability will be highlighted in this discussion as the estimation of relative permeability has been reported before, see, e.g., [9].

We start the simultaneous estimation by performing the *initial step*, estimating the relative permeabilities keeping the absolute permeability fixed at the harmonic mean value shown in Fig. 1. The first estimate of the relative permeabilities is shown in Fig. 2. The first estimate clearly deviate from the true curves, especially the oil relative permeability curve. The first estimate is plotted with 95% confidence intervals. We have also calculated the objective function, J, and number of runs, R, of the first estimate. These values are shown as the leftmost points in Figs. 5 and 6, respectively. The solid lines in these figures are the limits that the calculated values should approach. The horizontal lines around these lines indicate two standard deviations. The first relative permeability estimate is not accepted according to these statistics.

We have just illustrated that for this example, the harmonic mean value is not sufficient when estimating the relative permeabilities.

Before actually performing the first estimation of the absolute permeability in the successive approach, we have to decide which basis functions and how many to include in the basis matrix D. For the grid size we have, the number

Fig. 3. Synthetic experimental data. Pressure drop and oil production (Example 1).
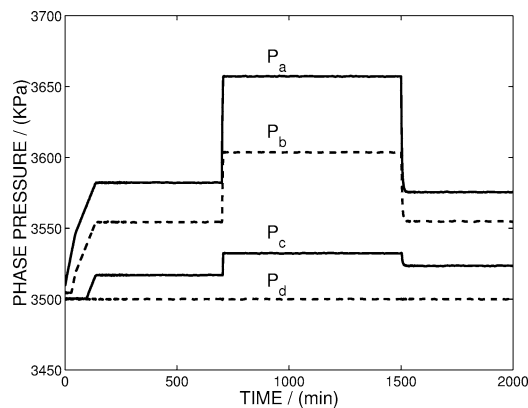
Fig. 4. Synthetic experimental data. Oil pressure measurements along the core (Example 1).
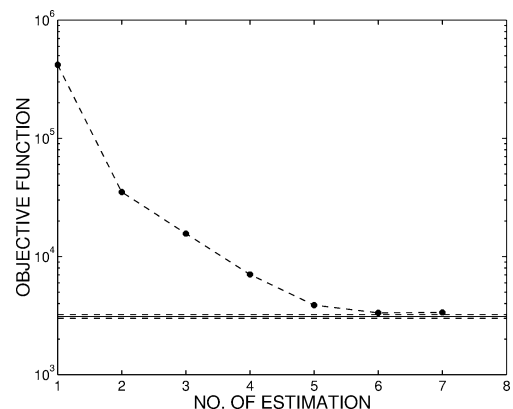

Fig. 5. Sum of squared residuals for each relative permeability estimation made in the successive approach (Example 1).
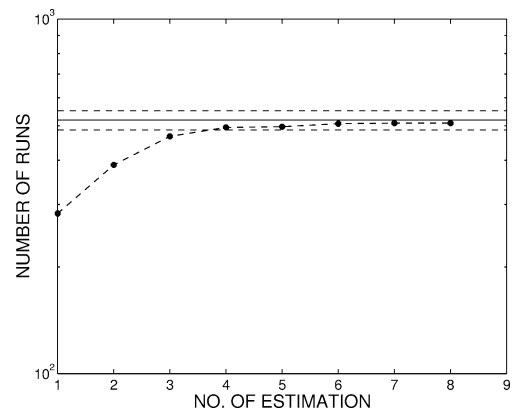

Fig. 6. Number of runs for each relative permeability estimation made in the successive estimation approach (Example 1).

of available basis functions is 32. Including all 32 would correspond to allowing different permeability in each grid cell. From earlier experience, we know that allowing this would give an unnecessary high uncertainty in the estimated parameters since the measured data hardly contain enough information for this high resolution. We will use a method, based on calculation of reduction potentials and L-curve methodology, which enables us to determine the smallest basis D sufficient to reconcile the measured data.

First, in determining D, we perform *step* 1. The point E1 in Fig. 7 corresponds to this estimate. Parameter sensitivities taken at this estimate are used to calculate reduction potentials. The first potentials are calculated by allowing one new basis function of the 31 available to be included; *step* 2. Fig. 8 shows the reduction potentials as a function of which basis function that is included in addition to basis function 1. Basis function 11 provides the highest reduction potential. Adding this basis function will result in estimating one value for the absolute permeability in grid blocks 1–10, and one value in grid blocks 11–32. The predicted objective function and the corresponding predicted uncertainty are given by the point P1a in Fig. 7.

Then, potentials are calculated by allowing combinations of two of the 31 available basis functions to be included in addition to basis function 1, *step* 2. The combination of three terms that provides the highest reduction potential corresponds to the point P1b in Fig. 7. (This will allow three absolute permeability values to be calculated, one for grid blocks 1–10, one for grid blocks 10–31, and one for grid block 32. Note that the basis D corresponding to point P1b does not necessarily have to be an extension of the basis corresponding to point P1a, even though that happened here.)

Next we perform *step* 3; the objective functions of point P1a and P1b in Fig. 7 are comparable. We see that including the basis functions of point P1b mainly increases the uncertainty compared to including the basis functions of point P1a, e.g., it is not necessary to evaluate further

extension of D. We perform *step* 4 using the basis functions corresponding to the point P1a. The dotted line in Fig. 1 shows the first estimate of the absolute permeability.

The estimate is not accepted according to calculated values of J and R. We proceed with a new estimation of the relative permeabilities, keeping the absolute permeabilities fixed; *step* 6. The second estimate of the relative permeabilities corresponds to the second estimate values in Fig. 5 and Fig. 6.

We then return to *step* 1, and proceed by the same approach as described above. The second time the absolute permeability was considered in the successive approach we derived the curve E2-P2a-P2b in Fig. 7, the third time we derived the curve E3-P3a-P3b, and so on. The number of estimations made, and the number of parameters used, in the successive approach of this example are given in Table 2.

For all the estimations made, J and R are calculated. (See Figs. 5 and 6 for the relative permeability estimations.) The successive approach terminated since the seventh absolute permeability estimate was comparable to the sixth, see *step* 5. (In seventh and the sixth estimation of the permeability, the same basis D was used, and the estimated functions were equal when considering two decimal places [mD].)

The final absolute permeability estimate is shown in Fig. 9. The basis D used when estimating the final absolute permeability corresponds to estimating one value for grid blocks 1–11, and one for grid blocks 12–32, i.e., the final estimate coincide with the true permeability partition-wise. The standard deviation of the estimate in both parts of the core is 0.03. Thus, the estimate is accurately determined and close to the true curves. J and R of this estimate are within four standard deviations of their limits.

Table 2
The number of estimations made, and the number of parameters estimated each time, for Example 1

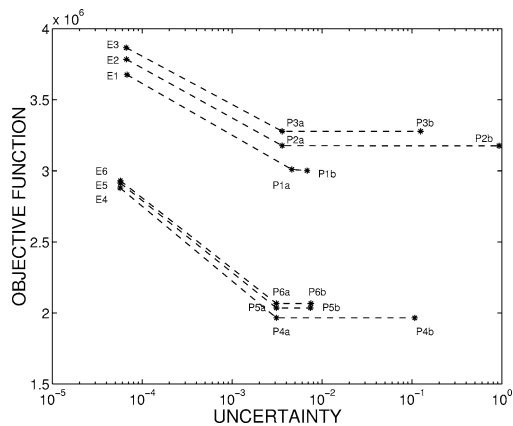| Estimation of	# of estimations	# parameters
Absolute permeability	7	2
Relative permeability	8	10

Fig. 7. Analysis of how many and which parameters to include in the estimation of absolute permeability. E is estimated value and P is predicted value. The E7-curve (not shown) almost coincides with the E6-curve. (Example 1).
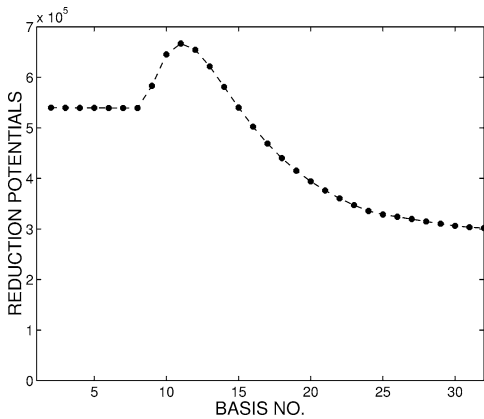

Fig. 8. Reduction potential as a function of which basis function to include in addition to basis function 1 (Example 1).

The final estimate of the relative permeability functions is shown in Fig. 10, and in Fig. 11 with logarithmic relative permeability axis. The estimated functions are given with 95% confidence intervals. The confidence intervals are narrow and contain the true curves. J and R of the final relative permeability estimate are within 2 standard
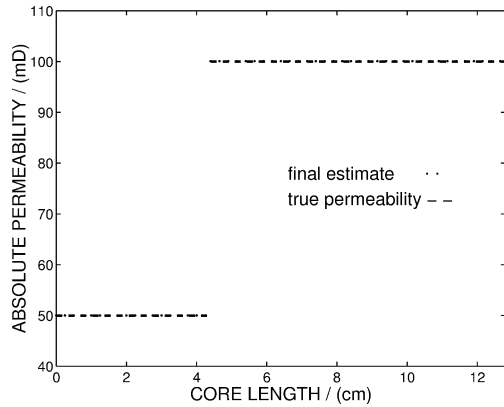

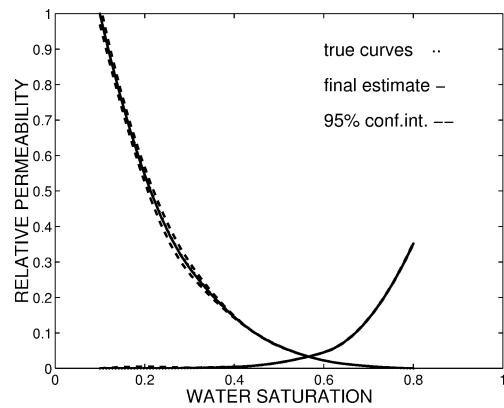Fig. 9. Absolute permeability. The true distribution and the final estimate (Example 1).

Fig. 10. Relative permeability. The true curve and the final estimate with 95% confidence interval (Example 1).
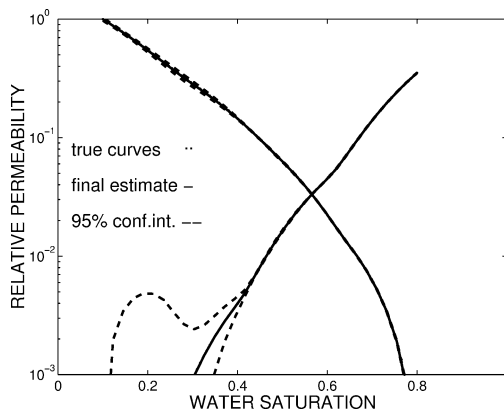
Fig. 11. Relative permeability. The true curve and the final estimate with 95% confidence interval. Plotted with logarithmic relative permeability axis (Example 1).

deviations of the limits; see the eight estimate values in Fig. 5 and Fig. 6.

Example 2. The true permeability used in this example is shown in Fig. 12. The core length and number of grids are the same as those used in Example 1. The true permeability is 50 mD in grid blocks 1–10, 200 mD in grid blocks 11–21, and 100 mD in grid blocks 22–32.

The true relative permeability functions are shown in Fig. 13, they are equal to those utilized in Example 1. All the other simulator input and settings, used when producing simulated experimental data, are also equal to those of Example 1, see Table 1. We use the same type of simulated experimental data as those shown in Fig. 3 and Fig. 4 in this example.

The simultaneous estimation starts by estimating the relative permeability functions keeping the absolute permeability fixed at the harmonic mean value shown in Fig. 12. Fig. 13 shows the first estimate of the relative permeability functions.

J and R of the first estimate are far from the limits; the first relative permeability estimate is not accepted. We
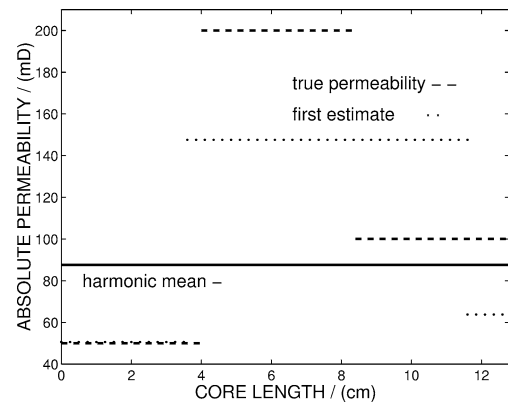

Fig. 12. Absolute permeability. The true distribution, the harmonic mean, and the first estimate (Example 2).
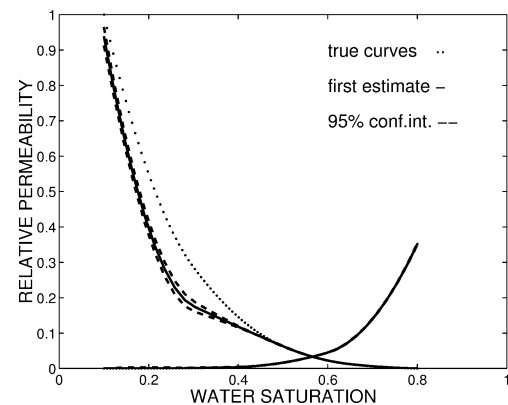

Fig. 13. Relative permeability. True curves, and first estimate with 95% confidence intervals (Example 2).

then turn to the absolute permeability keeping the relative permeabilities fixed at their first estimate.

We decide which and how many basis functions to include in the basis *D* by the same method utilized in Example 1. First, we estimate a mean value of the domain of definition; *step* 1. The point E1 in Fig. 14 corresponds to this estimate. From *step* 2, the point P1a in Fig. 14 corresponds to the candidate that provides the highest reduction potential when including one additional basis function. Including these two basis functions would provide a division of the grid in two parts, grid blocks 1–7 and grid blocks 8–32. The basis functions providing the highest reduction potential when including two additional basis functions correspond to the point P1b in Fig. 14. Selecting these three basis functions allows a subdivision in three parts, grid blocks 1–9, grid blocks 10–29, and grid blocks 30–32.

Step 3; the objective function of point P1a and P1b are not comparable, we therefore calculate reduction potentials including three additional basis functions. The candidate of these providing the highest reduction potential corresponds to the point P1c in Fig. 14. By studying the curve E1-P1a-P1b-P1c in Fig. 14, we decide to use the basis that corresponds to the point P1b when estimating the absolute permeability, while the basis corresponding to point P1c manly increases the uncertainty.

The first absolute permeability estimate is shown in Fig. 12. *J* and *R* are calculated, the values are far from the limits; this first estimate is not accepted.

We then estimate the relative permeabilities keeping the absolute permeability fixed at its first estimate; *step* 6. The

second estimate of the relative permeabilities is not accepted according to calculated values of *J* and *R*.

Table 3 gives a summary of the number of parameters used, and how many estimations that are made in the successive approach of this example. The estimation procedure terminated since the sixth absolute permeability estimate was within certain limits of the fifth estimate, see *step* 5.

The final absolute permeability estimate is shown in Fig. 15. Also in this example, the final estimate coincides with the true distribution partition-wise. The standard deviations of the estimates in grid blocks 1–10, 11–21, and 22–32 are 0.1, 0.1, and 0.9, respectively. The final estimate is accurate, close to the true distribution, and the calculated *J* and *R* of this estimate are within 2 standard deviations of their limits.

The final relative permeability estimate is shown in Fig. 16. This estimate is also accurately determined, and close to the true curves. *J* and *R* of this estimate are within 4 standard deviations of their limits.

Example 3. In this example we study the effect of absolute permeability distribution in each of the cores in the composite core of Example 2. The permeability variation

Table 3
The number of estimations made, and the number of parameters estimated each time, for Example 2

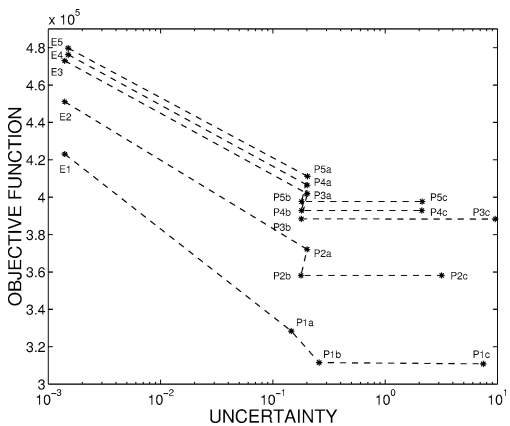| Estimation of	# of estimations	# parameters
Absolute permeability	6	3
Relative permeability	7	10

Fig. 14. Analysis of how many and which parameters to include in the estimation of absolute permeability. *E* is estimated value and *P* is predicted value. The E6-curve (not shown) almost coincides with the *E*5-curve. (Example 2).
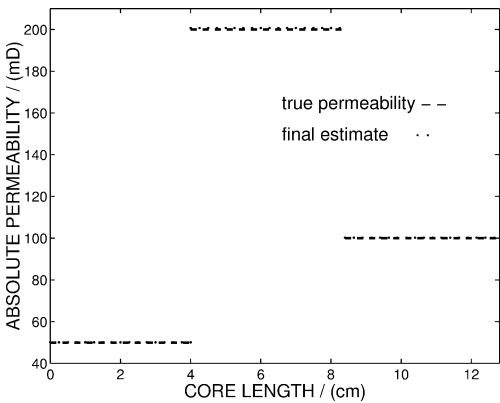

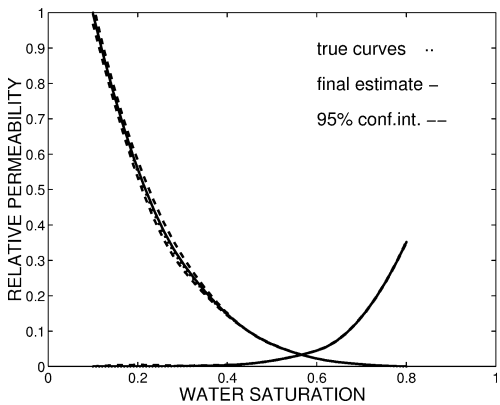Fig. 15. Absolute permeability. The true distribution and the final estimate (Example 2).

Fig. 16. Relative permeability. The true curve, the final estimate with 95% confidence interval (Example 2).

in each core is randomly chosen from a Gaussian distribution. In grid blocks 1–10 (the inlet core), the values are randomly collected from a Gaussian distribution with mean value 50 mD and standard deviation 5 mD. For the middle core of the composite, grid blocks 11–21, the mean value and standard deviation of the Gaussian distribution are 200 mD and 20 mD, respectively. For the outlet core, grid blocks 22–32, the mean is 100 mD and the standard deviation is 10 mD for the Gaussian distribution. Fig. 17 shows the resulting absolute permeability distribution. All the other settings, (relative permeabilities, core length, etc.), is equal to those used in Example 2.

By using the estimation algorithm in section 4.4 we perform the simultaneous estimation. Fig. 18 shows the first relative permeability estimate. This is obtained by keeping the absolute permeability fixed at the harmonic mean given in Fig. 17. J and R of the first estimate are far from their limits. We then estimate the absolute permeability keeping the relative permeabilities fixed at their first estimate.

We decide which and how many basis functions to use in the absolute permeability estimation by the same method as described in the two previous examples. In Fig. 19, the curve E1-P1a-P1b-P1c is used to select the basis for the first estimation. The basis functions corresponding to the point
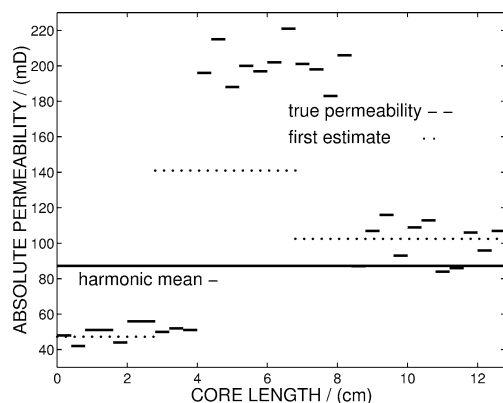
P1b are chosen, this corresponds to a subdivision of the grid in three parts, grid blocks 1–7, grid blocks 8–17, and grid blocks 18–32. The first absolute permeability estimate is shown in Fig. 17. For this estimate, J and R are far from their limits, i.e., the estimate is not accepted.

Table 4 gives a summary of the number of parameters used, and how many estimations that are made in this example. The simultaneous estimation terminated since the solution criteria for the final estimates are satisfied (*step* 6).

The final absolute permeability estimate is given in Fig. 20. J and R of this estimate are within two standard deviation of their limits. The standard deviation is 0.1 for all the three permeability values of the final estimate. The final estimate does not match the fine scale variation within

Table 4
The number of estimations made, and the number of parameters estimated each time, for Example 3

Estimation of	# of estimations	# parameters
Absolute permeability	6	3
Relative permeability	7	10

Fig. 17. Absolute permeability. The true distribution, the harmonic mean, and the first estimate (Example 3).

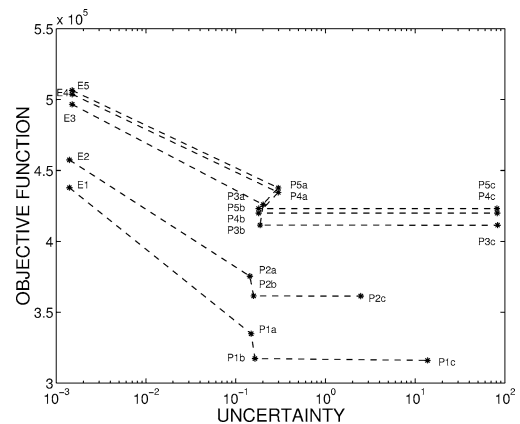Fig. 19. Analysis of how many and which parameters to include in the estimation of absolute permeability. E is estimated value and P is predicted value. The E6-curve (not shown) almost coincides with the E4-curve (Example 3).

Fig. 18. Relative permeability. True curves, and first estimate with 95% confidence intervals (Example 3).
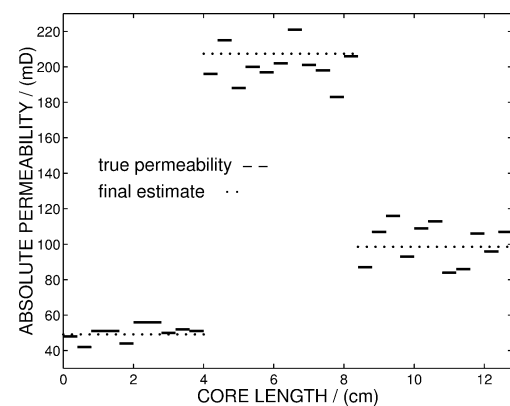

Fig. 20. Absolute permeability. The true distribution and the final estimate (Example 3).
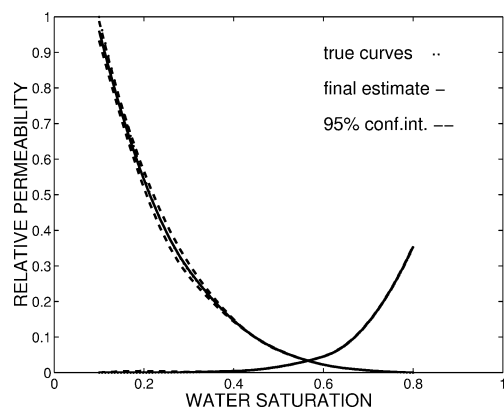
Fig. 21. Relative permeability. The true curve, the final estimate with 95% confidence interval (Example 3).

the individual cores, but it does match the coarse scale main jumps of the true permeability of the composite. This final absolute permeability estimate is used when estimating the final relative permeabilities shown in Fig. 21. The final relative permeability estimate is also accepted according to the statistical criteria; the calculated J and R are within two standard deviations of their limits.

This example shows that it can be sufficient to account for the main absolute permeability variation in order to get acceptable relative permeability estimates.

6. Conclusions

(1) Utilizing the harmonic mean value of the absolute permeability may seriously affect the estimation of relative permeabilities.

(2) We have presented a method where the absolute and relative permeabilities are estimated simultaneous through a successive approach.

(3) The absolute permeability is given a multiscale representation in this work. A new method for searching for optimal partitioning when using such representations is presented. The method is based on calculations of predicted reduction in the objective function value and predicted parameter uncertainties. It is fast and inexpensive from a computational point of view.

(4) Three examples are provided to demonstrate the successive estimation method. For the 1D heterogeneous absolute permeability distribution studied in these examples, the method provides acceptable estimates of both absolute and relative permeability.

(5) We have demonstrated that fine scale permeability variations within a core sample will not influence the estimation of the relative permeabilities provided that the scale of variation is sufficiently small compared to the scale of the core sample.

References

[1] K. Aziz, A. Settari, Petroleum Reservoir Simulation, Applied Science Publisher, New York, 1979.

[2] Y. Bard, Nonlinear Parameter Estimation, Academic Press, Washington, DC, 1974, p. 201.

[3] G. Chavent, J. Liu, Multiscale parameterization for the estimation of a diffusion coefficient in elliptic and parabolic problems, in: Proc. Fifth IFAC Symposium on Control of Distributed Parameter Systems, 1989.

[4] P.E. Gill, W. Murray, M.H. Wright, Practical Optimization, Academic Press, London, 1981.

[5] A.-A. Grimstad, T. Mannseth, J.-E. Nordtvedt, G. Nævdal, Reservoir characterization through scale splitting, in: Proc. Symp. of the Seventh European Conference on Mathematics of Oil Recovery (ECMOR VII), 2000.

[6] A.A. Grimstad, K. Kolltveit, J.-E. Nordtvedt, A.T. Watson, T. Mannseth, A. Sylte, The uniqueness and accuracy of porous media multiphase properties estimated from displacement experiments, in: Proc. SCA International Symposium, SCA-9709, 1997.

[7] Y. Guo, J.-E. Nordtvedt, H. Olsen, Development and Improvement of CENDRA+, Report RF-183/93, Confidential.

[8] P.C. Hansen, Analysis of discrete ill-posed problems by means of the L-curve, SIAM Review 34 (4) (1992) 561–580.

[9] A.T. Kerig, P.D. Watson, A new algorithm for estimating relative permeabilities from displacement experiments, SPE Reservoir Engineering 2 (1987) 103–112.

[10] R. Kulkarni, A.T. Watson, J.-E. Nordtvedt, A. Sylte, Two phase flow in porous media: Property identification and model validation, AIChE J. 44 (11) (1998) 2337–2350.

[11] T. Mannseth, J.-E. Nordtvedt, G. Nævdal, Optimal management of advanced wells through fast updates of the near-well reservoir model, in: Proc. Symp. the Seventh European Conference on the Mathematics of Oil Recovery (ECMOR VII), Baveno, Italy, September, 2000.

[12] J.-E. Nordtvedt, H. Urkedal, E. Ebeltoft, K. Kolltveit, E.B. Petersen, A. Sylte, R. Valestrand, The significance of violated assumptions on core analysis results, in: Proc. Symp. SCA International Symposium, SCA-9931, 1999.

[13] L.L. Schumaker, Spline Functions: Basic Theory, Wiley, New York, 1981.

[14] A. Sylte, E. Ebeltoft, A.A. Grimstad, R. Kulkarni, J.-E. Nordtvedt, A.T. Watson, Design of two-phase flooding experiments, Inverse Problems in Engineering, to appear.

[15] H. Urkedal, E. Ebeltoft, J.-E. Nordtvedt, A.T. Watson, A new design of steady-state type experiments for simultaneous estimation of two-phase flow functions, in: Proc. Symp. SPE Reservoir Evaluation and Engineering, SPE-64532, 2000.

[16] H. Urkedal, Design of multiphase flow experiments, Dr. Scient Thesis, Department of Physics, University of Bergen, 1998.

[17] R. Valestrand, The impact of permeability heterogeneities on flow function estimation, Cand. Scient. Thesis in Physics, Dept. of Physics, University of Bergen, Norway, 1999.

[18] A.T. Watson, P.C. Richmond, P.D. Kerig, T.M. Tao, A regression based method for estimating relative permeabilities from displacement experiments, Proc. Symp. SPE Reservoir Engineering 3 (1988) 953–958.

[19] S. Weisberg, Applied Linear Regression, Wiley, New York, 1985.